Original Paper

European Surgical Research

Eur Surg Res 2011;47:240–247
DOI: 10.1159/000333087

Received: July 1, 2011
Accepted after revision: September 12, 2011
Published online: November 2, 2011

In vivo Imaging of Bile Accumulation and Biliary Infarction after Common Bile Duct Ligation in Rats

J.-C. Harnoss[a, b] C.D. Heidecke[c] B. Vollmar[a] C. Eipel[a]

[a]Institute for Experimental Surgery, University of Rostock, Rostock, [b]Department of General, Visceral and Transplantation Surgery, University of Heidelberg, Heidelberg, and [c]Department of General and Visceral Surgery, University of Greifswald, Greifswald, Germany

Key Words
Common bile duct ligation · Cholestasis · Fibrosis · In vivo imaging · Autofluorescence

Abstract
Obstructive cholestasis is caused by mechanical constriction or occlusion leading to reduced bile flow. Serious complications such as jaundice and even death may follow. Little is known about the initial phase of cholestasis and its consequences for the hepatic microarchitecture. This in vivo study aimed to characterize the nature and kinetics of developing obstructive cholestasis and focused on areas with biliary stasis and infarction by visualizing the autofluorescence of bile acids using intravital microscopy of the liver over a period of 30 h after bile duct ligation in rats. The innovation resided in performing fluorescence microscopy without applying fluorescent dyes. In animals subjected to obstructive cholestasis, the most significant changes observed in vivo were the concomitant appearance of (1) areas with bile accumulation increasing in size (6 h: 0.163 ± 0.043, 18 h: 0.180 ± 0.086, 30 h: 0.483 ± 0.176 mm^2/field) and (2) areas with biliary infarction (6 h: 0.011 ± 0.006, 18 h: 0.010 ± 0.004, 30 h: 0.010 ± 0.050 mm^2/field) as well as (3) a relation between the formation of hepatic lesions and enzyme activity in serum. The sequential in vivo analysis presented herein is a new method for the in vivo visualization of the very early changes in the hepatic parenchyma caused by obstructive cholestasis.

Introduction

Obstructive cholestasis is caused by a structural or mechanical obstruction of bile flow in the extrahepatic bile duct. The common reasons include choledocholithiasis and malignant processes such as cholangiocarcinoma and pancreatic cancer. It is a serious illness that may lead to jaundice and even death unless the obstructive lesion is removed or the bile duct is bypassed [1]. The pathological process of developing liver cirrhosis is best characterized in animals studied by common bile duct ligation (CBDL). CBDL impairs bile formation and excretion into the intestine. This impairment results in elevated blood levels of several bile solutes such as cholesterol, bile acids and bilirubin that are normally excreted into bile [2, 3].

The pathophysiology of obstructive cholestasis represents an almost inconceivably complex network of interacting cells, fibrogenic mediators, and extracellular matrix (ECM) molecules [4]. Dramatic improvements in cell

KARGER
Fax +41 61 306 12 34
E-Mail karger@karger.ch
www.karger.com

0014–312X/11/0474–0240$38.00/0

Accessible online at:
www.karger.com/esr

Christian Eipel, PhD
Institute for Experimental Surgery, University of Rostock
Schillingallee 69a
DE–18057 Rostock (Germany)
Tel. +49 381 494 2503, E-Mail christian.eipel@uni-rostock.de

and molecular biological techniques now permit detailed analysis of the composition, structure, immunology and histological localization of the individual components of the ECM. Dissection of the cellular and molecular pathobiology of ECM deposition includes the identification of the cellular sources of specific ECM components as well as the definition of humoral factors and regulatory loops underlying both the amplification and degradation pathways of ECM molecules during fibrogenesis [5].

Besides the molecular aspects of fibrogenesis, which have been studied in depth, there is a lack of information about the initial steps of hepatic microarchitectural and microvascular changes during cholestasis in vivo. Using intravital microscopy in a rat model of developing cholestasis, the present study shows the nature, extent and relevance of biliary stasis and necrosis in the process of hepatic organ remodeling in vivo.

Methods

Animal Model

Experiments were performed in accordance with the German legislation on the protection of animals and the *Guide for the Care and Use of Laboratory Animals* (NIH publication No. 86-23, revised in 1985). A total of 20 male Sprague-Dawley rats (Charles River, Fa. Wiga, Sulzfeld, Germany, body weight about 280 g) were anesthetized with an intraperitoneal injection of pentobarbital sodium (50 mg/kg body weight), and laparotomy was performed for CBDL (n = 17). Control rats underwent an identical surgical procedure without CBDL, however (n = 3). All animals were allowed to recover from anesthesia and surgery under a red warming lamp and were housed in single cages in an environmentally controlled room with a 12-hour light-dark cycle with free access to water and standard pellet food. The animals were studied at 6 h (n = 4), 18 h (n = 3) and 30 h (n = 3) after CBDL. Seven animals (3 from the 6-hour group, 2 from the 18-hour group, and 2 from the 30-hour group) died before the treatment period was completed.

In vivo Studies

For intravital microscopy, the animals were anesthetized with an intraperitoneal injection of pentobarbital sodium (50 mg/kg body weight) at the respective time points after CBDL and placed in the supine position on a heating pad for maintenance of body temperature at 37°C. After tracheotomy, the right carotid artery was exposed and cannulated for heart rate and blood pressure monitoring (PE-50; ID 0.58 mm; Portex, Hythe, UK). After transverse and longitudinal laparotomy, the liver was prepared for intravital fluorescence microscopy by placing the left lobe on a plasticine disk held by an adjustable stage that was attached to the heating pad [6]. Thereby, the lower surface of the liver was horizontal to the microscope, which guaranteed an adequate homogeneous focus level for the microscopic procedure of the liver surface. In addition, adjustment of the plasticine disk allowed us to avoid mechanical obstruction of feeding and draining macrovessels and to minimize respiratory movements of the lobe. The exposed area of the left liver lobe was immediately covered with a glass slide to prevent tissue drying and the influence of ambient oxygen. At the end of the experiments, i.e. after intravital microscopic analysis of the hepatic microstructure, the animals were killed by exsanguination. Venous blood samples were taken for spectro-photometric determination of serum activities of aspartate aminotransferase (AST), alanine aminotransferase (ALT), total bilirubin (BILI-T) and direct/conjugated bilirubin (BILI-D). Indirect/unconjugated bilirubin (BILI-ID) was determined by subtracting BILI-D from BILI-T.

Intravital Fluorescence Microscopy

In vivo microscopy was performed using a modified fluorescence microscope (Axio-Tech Vario; Zeiss, Jena, Germany) and the epi-illumination technique with a 100-watt mercury lamp. Microscopic images were registered by a charge-coupled device video camera (FK 6990-IQ; Pieper, Berlin Germany) and recorded on video tape for subsequent off-line evaluation. Using a ×10 objective (10×/0.30, Zeiss), or a water immersion objective (20×/0.5, Zeiss), magnifications of ×300 and ×700 were achieved on the video screen (PVM-1442 QM, diagonal: 330 mm, Sony). By means of different filter sets, images of autofluorescence of the hepatic surface (10–15 observation areas per animal) were taken. For detection of autofluorescent areas with bile accumulation or biliary necrosis, blue fluorescence epi-illumination (excitation/emission wavelengths: 450–490 nm/>520 nm) was used. Ultraviolet epi-illumination (330–390 nm/>430 nm) allowed for observation of multiple patchy fluorescent activities derived from vitamin A in Ito cells [7] and completely eliminated vitamin A autofluorescence within about 20 s of exposure due to its rapid photobleaching property [7].

Quantitative Analysis

Quantitative analysis was performed off-line by a computer-assisted image analysis system (CapImage; Zeintl, Heidelberg, Germany). The extent of biliary accumulation and/or biliary infarction was (1) planimetrically quantified as areas per observation field (given in square millimeters per visual field) and (2) counted as number of areas with (a) biliary accumulation, (b) biliary infarction or (c) combined lesions (each given as number per visual field) using the blue epi-illuminated microfluorographic images. The number of positive vitamin A sites was calculated as number per square millimeter in (1) unaffected periportal fields and (2) affected periportal fields with lesions such as biliary stasis or infarction using ultraviolet epi-illuminated microfluorographic images.

Histology

Liver tissue samples were fixed in 4% phosphate-buffered formalin for 2–3 days and embedded in paraffin. From the paraffin-embedded tissue blocks, 5-μm sections were cut and stained with hematoxylin and eosin (HE) for routine histology and examined by light microscopy and blue fluorescence epi-illumination (excitation/emission wavelengths: 450–490 nm/>515 nm).

Statistics

Data are presented as means ± SEMs. After performing a normality test, statistical differences at different time points after CBDL versus values of control rats without CBDL were determined by one-way analysis of variance followed by a Holm-Sidak comparison test. Data were considered significant when $p < 0.05$.

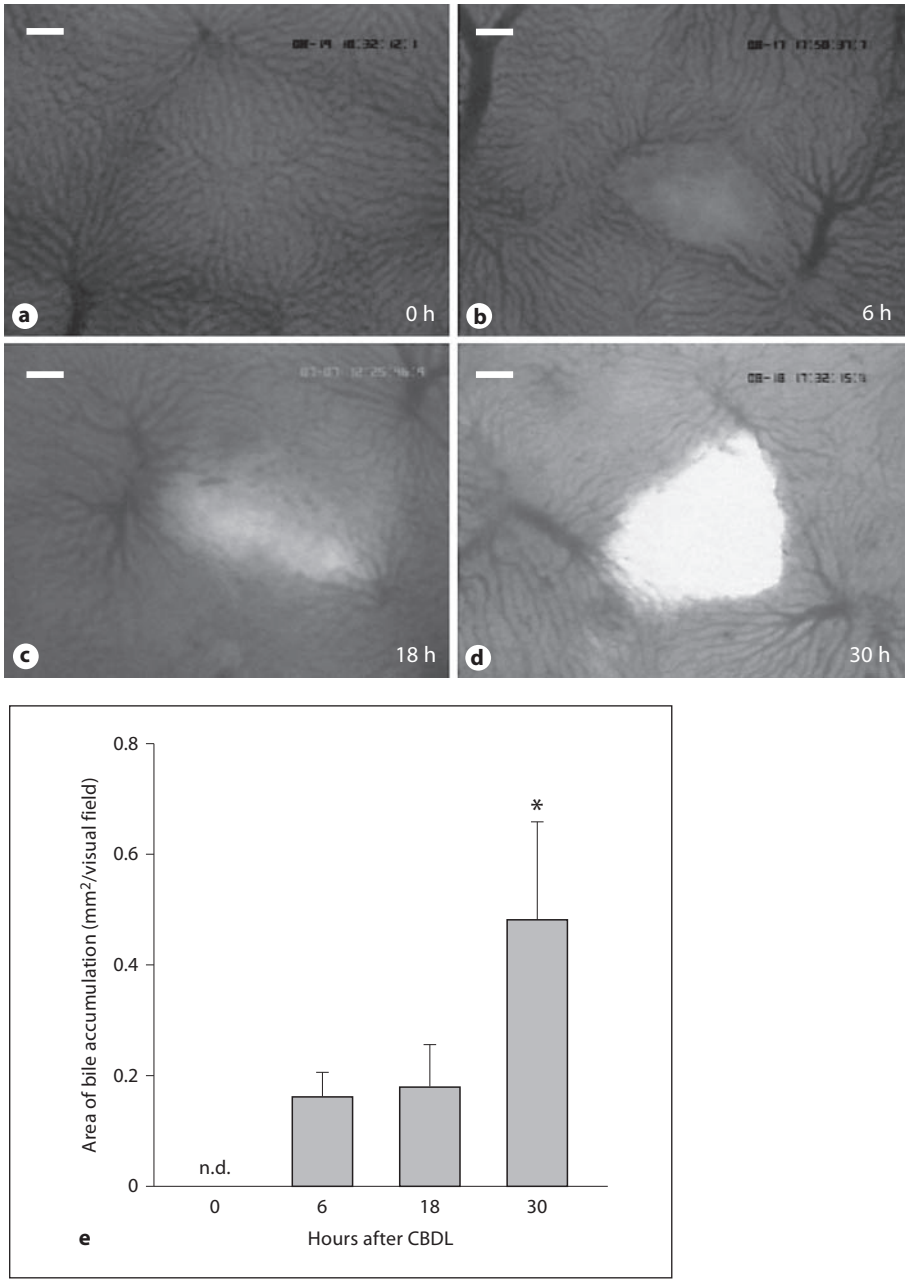

Fig. 1. Intravital fluorescence microscopic images of periportal fields in an untreated control liver (**a**) and liver at 6 h (**b**), 18 h (**c**), and 30 h (**d**) after CBDL. Whereas the morphology of the liver parenchyma is normal in the control animal (**a**), initial changes of hepatic parenchyma with pronounced accumulation of bile originating from the periportal field are apparent already after 6 h of cholestasis (**b**), increasing in size with time (**c**) and finally occupying a whole triangular portal field (**d**). Blue-light epi-illumination. Bars represent 100 μm. **e** Quantitative analysis revealed a progressively increasing bile accumulation after CBDL. Means ± SEM, * $p < 0.05$ vs. 0 h.

Results

Gross Findings

The average body weight of the control animals and the animals with cholestasis at 6, 18 and 30 h did not differ (284 ± 7, 312 ± 22, 335 ± 45 and 268 ± 20 g, respectively). At laparotomy of cholestatic animals, neither changes of liver surfaces nor signs of portal hypertension, namely splenomegaly, ascites, and increased diameter of the portal vein and its intestinal afferents were observed. Calculation of liver to body weight ratios indicated increasing liver hypertrophy with values of 3.7 ± 0.2, 3.5 ± 0.4 and 4.1 ± 0.3% after 6, 18 and 30 h CBDL compared with the corresponding liver to body weight ratio of control animals (2.5 ± 1.4%).

Intravital Microscopic Morphology

Intravital observation of biliary autofluorescence (450–490 nm/>520 nm) revealed remarkable differences regarding the extent and quality of initially occurring le-

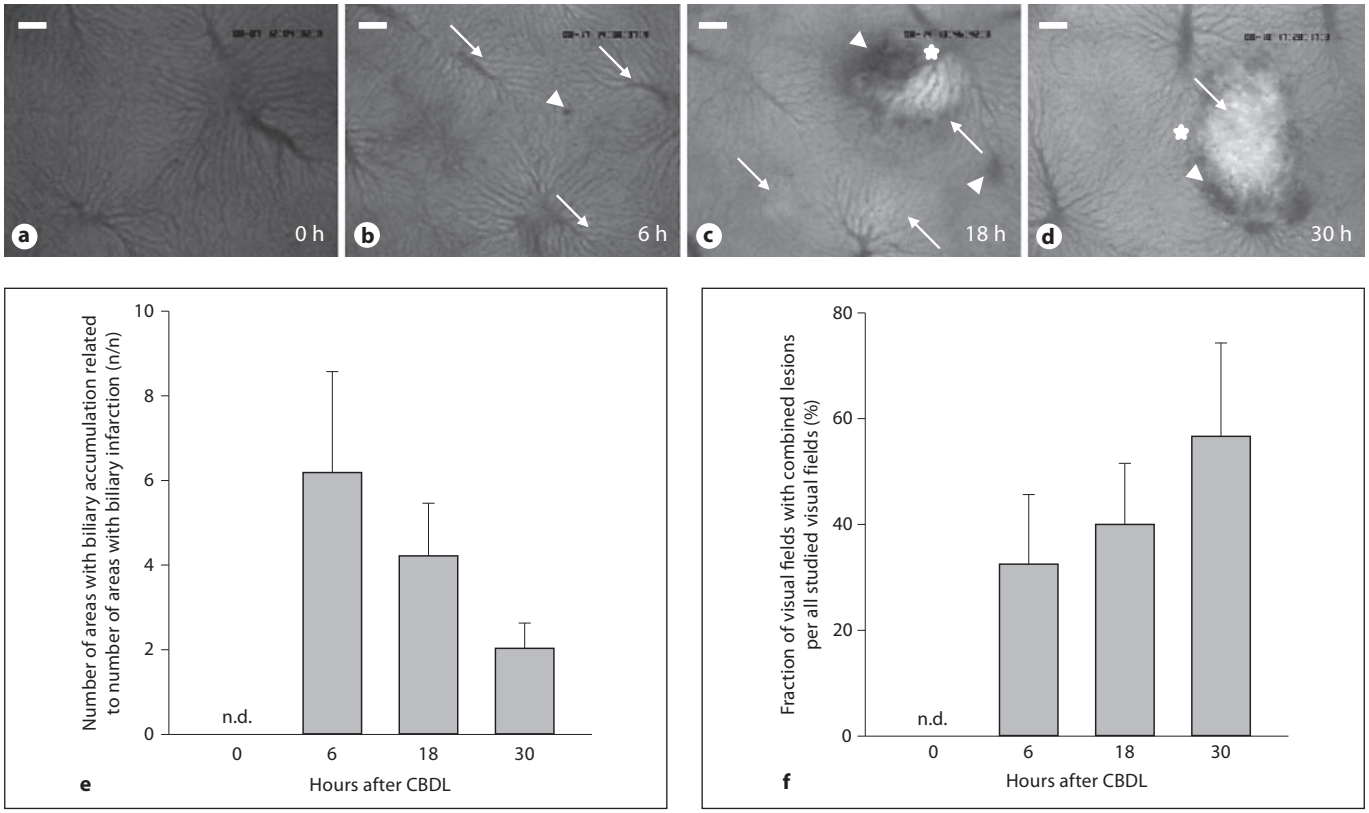

Fig. 2. Intravital fluorescence microscopic images of liver parenchyma before (**a**), as well as 6 h (**b**), 18 h (**c**), and 30 h (**d**) after CBDL. The liver of a control animal reveals no biliary lesions (**a**), while after CBDL, areas with bile accumulation (arrows), biliary stasis (arrowheads), and combined lesions (asterisk) could be observed (**b**, **c**). At 30 h after CBDL, the whole liver parenchyma is brightened up (**d**) in comparison to the control (**a**). Blue epi-illumination. Bars represent 100 μm. Quantitative analysis shows a decrease in the relation of area count with bile accumulation to area count with biliary infarction from 6 to 18 and 30 h after CBDL, respectively (**e**). In parallel, there is an increasing fraction of visual fields presenting areas with both bile accumulation and infarction (**f**). Means ± SEM.

sions between control and CBDL animals as well as between cholestatic animals at different time points after CBDL (fig. 1). Cumulated bile was observed very early in periportal fields of animals 6 h after CBDL (0.163 ± 0.043 mm^2/visual field). The extent of bile accumulation increased by more than 10 and 160%, respectively (0.180 ± 0.086 mm^2/visual field and 0.483 ± 0.176 mm^2/visual field) at 18 and 30 h after CBDL. As expected, hepatic defects such as dark areas of infarction or bile-associated autofluorescence in areas of biliary stasis could not be observed in control animals (fig. 1). Infarction areas presenting with poor autofluorescence in blue-light epi-illumination were observed as solitary, periportal lesions in animals at 6 h after CBDL (fig. 2b). Although the size of areas with cholestatic bile was clearly increasing, the number of lesions with accumulated bile in relation to the number of infarction sites was remarkably decreasing over time by more than 50% (fig. 2e). This might be explained by the concomitant observation that 6, 18 and 30 h after CBDL, combined lesions showing both biliary stasis and infarction were increasingly occurring in 33 ± 13, 40 ± 12 and 57 ± 18% of visual fields, respectively (fig. 2f). The whole hepatic parenchyma revealed obviously increasing bile-associated autofluorescence in blue-light epi-illumination with increasing duration of cholestasis.

No remarkable differences were observed between the CBDL and control animals with respect to acinar distribution of vitamin A-associated autofluorescence. The mean number of cells showing vitamin A-associated autofluorescence was unchanged in the unaffected periportal fields of animals at 6 h (1,175 ± 172/mm^2) and 18 h after CBDL (1,347 ± 162/mm^2) compared to control animals (1,380 ± 169/mm^2). However, in periportal fields with lesions such as biliary stasis or infarction, the mean

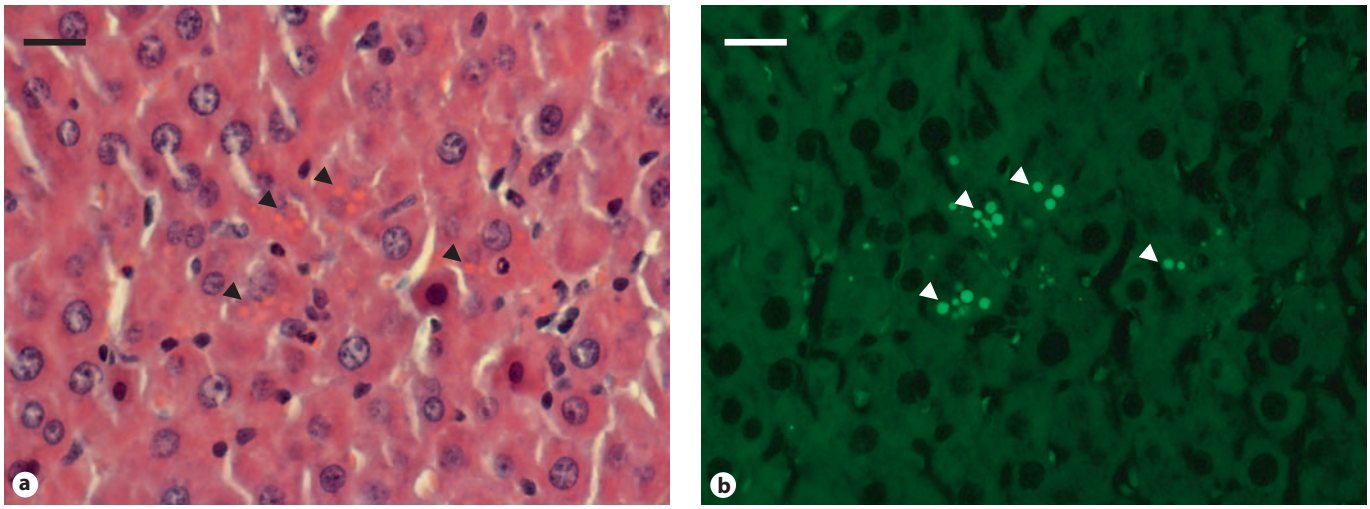

Fig. 3. HE histology (**a**) and blue fluorescence epi-illumination (**b**) of the identical liver section at 6 h after CBDL. Deposits of intracytoplasmic bile pigments could be observed (arrowheads). Bars represent 20 μm.

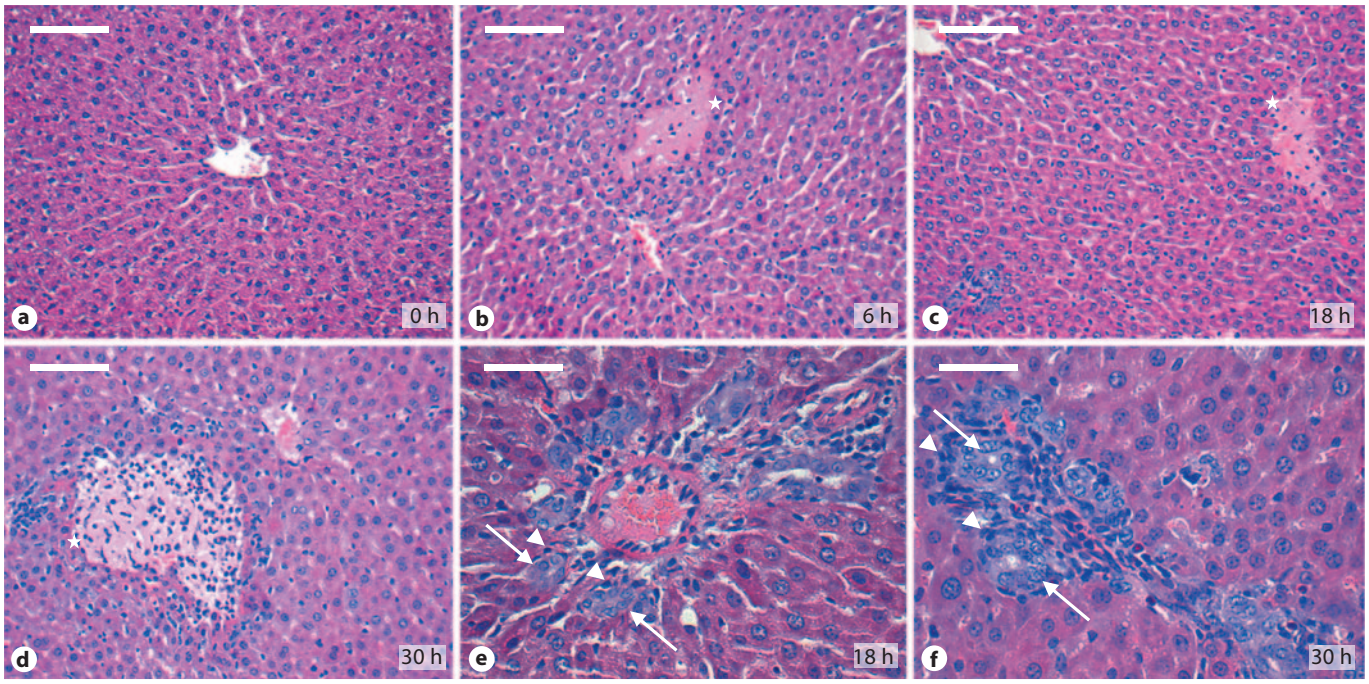

Fig. 4. HE-stained liver sections of an untreated control animal (**a**) and animals at 6 h (**b**), 18 h (**c**, **e**) and 30 h (**d**, **f**) after CBDL. Whereas regular liver histology was found in control animals (**a**), severe confluent necrotic fields (asterisks) are apparent after CBDL (**b–d**). At 18 h (**e**) and 30 h (**f**) after CBDL, proliferating bile ductules (arrows) surrounded by neutrophils (arrowheads) may be observed. Bars represent 100 μm (**a–d**) or 50 μm (**e**, **f**).

number of cells with vitamin A-associated autofluorescence was markedly lower in animals at 6 h (772 ± 118/mm^2) and 18 h after CBDL (617 ± 24/mm^2) compared to control animals. Because of enhanced biliary autofluorescence in the whole hepatic parenchyma at 30 h after CBDL, clear identification of unaffected periportal fields was not possible any more.

Liver Histology

In HE-stained liver sections, deposits of intracytoplasmic bile pigments could already be observed at 6 h after CBDL (fig. 3a). By blue fluorescence epi-illumination of the identical field, bile accumulation became even more visible (fig. 3b). Whereas the microarchitecture of liver histology was found regularly in control animals (fig. 4a), we already observed severe lesions such as confluent necrotic fields in CBDL animals (fig. 4b–d). Furthermore, the HE-stained liver sections showed proliferating bile ductules surrounded by neutrophils at 18 and 30 h after CBDL (fig. 4e, f).

Plasma Analysis

Concomitantly, liver enzyme activities in serum increased more than 8-fold (AST: 1,059 ± 188 U/l) and 9-fold (ALT: 413 ± 96 U/l) already at 6 h after CBDL compared with values of control animals (AST: 131 ± 7 U/l; ALT: 43 ± 5 U/l). Serum AST activity did not further increase at later time points with enduring cholestasis (18 h CBDL, AST: 1,085 ± 250 U/l; ALT: 516 ± 181 U/l; 30 h CBDL, AST: 1,047 ± 194 U/l; ALT: 540 ± 72 U/l; fig. 5). Compared to control animals (1.73 ± 0.16 μmol/l), serum BILI-T activity was found to steadily increase by more than 35-fold within 30 h after CBDL (6 h: 27.2 ± 2.1, 18 h: 47.4 ± 5.8, 30 h: 61.6 ± 9.8 μmol/l). After CBDL, serum BILI-D activity revealed a constant increase (6 h: 15.8 ± 2.3, 18 h: 11.4 ± 1.6, 30 h: 37.4 ± 9.2 μmol/l), whilst the activity of unconjugated bilirubin was found to be almost 6-fold increased at 6 h after CBDL (11.4 ± 1.6 μmol/l), reached a steady state between 6 and 18 h (10.0 ± 3.9 μmol/l) and raised again between 18 and 30 h by about 68% (16.7 ± 3.2 μmol/l; fig. 6).

Discussion

Cholestasis is a clinically significant entity because of its association with significant morbidity and sometimes mortality [8]. Treatments for cholestasis remain largely nonspecific and often ineffective [9]. Cholestasis is attributed to stagnation of toxic hydrophobic bile acids and is accompanied with cytoplasmic changes in periportal hepatocytes [10]. Elevated serum and tissue levels of bile salts and other toxic compounds during cholestasis may cause mitochondrial damage, apoptosis or necrosis in susceptible cell types [3, 11]. Bilirubin, the principal breakdown product of hemoglobin and other hemeproteins, is normally excreted with the bile. Impaired bile excretion in liver disease or in instances of obstruction in the biliary duct system causes a rise in the plasma bilirubin concentration that eventually leads to clinical jaundice. In the present study, hepatic retention of bilirubin pigments during CBDL-induced obstructive cholestasis was investigated for the first time in vivo. For this purpose, we used the autofluorescence of bilirubin most probably emitted by a tetrapyrrole prosthetic group [12]. The innovation resides in performing fluorescence microscopy without applying fluorescent dyes. The faint autofluorescence of the liver parenchyma enabled clear visualization of the hepatic microvascular structure and demonstration of the kinetics of morphological changes caused by accumulation of bilirubin in hepatocytes, bile canaliculi and bile ducts from which hepatic parenchymal damage takes its origin and to correlate these changes with hepatobiliary function at a very early stage of obstructive cholestasis.

As expected, we observed increasing biliary autofluorescence during progression of cholestasis, corresponding to enhanced bilirubin pigment storage in the cytoplasm of hepatocytes as an initially consequence of cholestasis. The increase in cytoplasmatic autofluorescence may be explained by an immediate downregulation of canalicular excretion transporters as a consequence of mechanical impedance of bile flow [13]. In parallel, a decreased uptake of bile solutes from sinusoids by reducing inward transporters keeps more solutes in the sinusoids and hence in the circulation [13]. As a marker for reduced hepatic uptake, we found an increase in serum BILI-ID activity along with significantly increased bile accumulation.

Bile lakes were reported to occur in obstructive jaundice due to bile acid accumulation, and their appearance in the periportal area is characteristic of severe bile duct obstruction [14]. The toxic action of bile is assumed to cause bile infarction in extrahepatic biliary obstruction [15]. In our intravital fluorescence microscopic approach, bile infarcts appear as nonfluorescent areas in direct vicinity to bile lakes. Our in vivo data showed the incidence of bile infarcts already 6 h after CBDL. Whereas at 6 h after CBDL these areas mostly appear as solid infarcts, 18 and 30 h after onset of obstructive cholestasis, we found a raised count of areas with combined lesions (bile lakes and bile infarcts) as typical parenchymal damage following

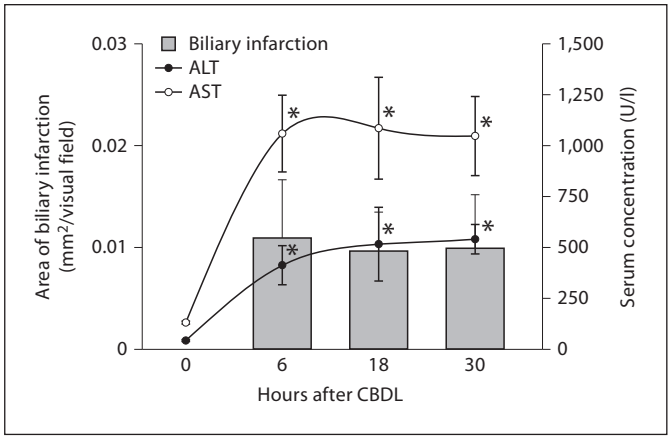

Fig. 5. Extent of biliary infarction in livers of animals at 6, 18 and 30 h after CBDL compared to control animals and its relation to the serum AST and ALT activity. Whereas no infarction sites were found in normal livers, infarction areas of nearly the same extent could be observed at all time points after CBDL. Consistently, serum AST and ALT activity increased more than 8-fold (AST) and 9-fold (ALT) at 6 h after CBDL and remained elevated at later time points. Means ± SEM, * $p < 0.05$ vs. 0 h.

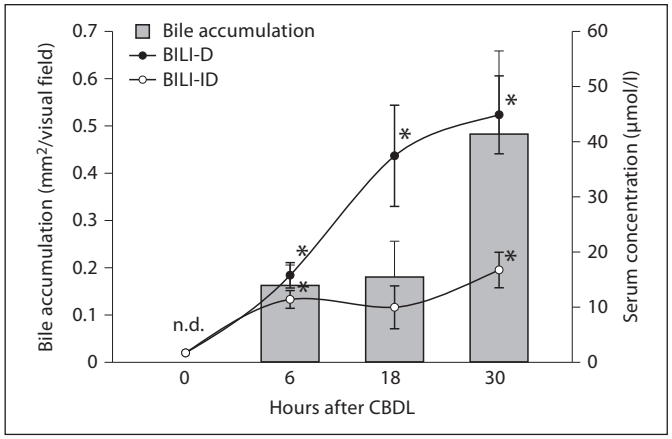

Fig. 6. Extent of bile accumulation in livers of animals at 6, 18 and 30 h after CBDL compared to control animals and its relation to serum BILI-D and BILI-ID activity. Whereas no areas of accumulated bile were found in normal livers, these areas were continuously increasing after CBDL. In parallel, serum BILI-D activity steeply increased after CBDL. Serum BILI-ID activity displayed an increase at 6 h after CBDL without a further rise at later time points. Means ± SEM, * $p < 0.05$ vs. 0 h.

thrombosis and thus rupture of bile canaliculi (fig. 2). Concomitantly, we histologically observed proliferating bile ductules with an adjacent inflammatory reaction representing severe lesions already occurring at 18 and 30 h after CBDL. Combined defects were often located in portal and para-periportal areas. It might be speculated that within the first 6 h after CBDL, infarcts mainly occur in areas affected by lytic cell necrosis after cytoplasmic cholestasis whereas subsequently, infarction preponderantly follows canalicular thrombosis. Our results are further confirmed by increasing activity of hepatic transaminases in serum which suggest the occurrence of cytoplasmic and mitochondrial damage within the first 6 h of cholestasis.

It has been reported that Ito cells (hepatic stellate cells) are the principal effectors of liver fibrogenesis [16]. As disease progresses, these vitamin A-rich cells become activated, proliferate and produce ECM [17, 18]. We did not observe any difference between CBDL animals and controls with respect to acinar distribution of vitamin A-associated autofluorescence or the mean number of hepatic Ito cells in inconspicuous periportal fields. Nevertheless, our present data show lower vitamin A-associated autofluorescence in affected periportal fields with lesions such as biliary stasis or infarction in rats 6 and 18 h after CBDL. These findings suggest that imaging of bile acids by intravital fluorescence microscopy may be used for early, reliable detection and classification of hepatic pathophysiological changes after the onset of obstructive cholestasis.

Over a period of weeks or months, untreated cholestasis causes lytic cell necrosis. As long as the cause of biliary obstruction persists, biliary fibrosis and cirrhosis may occur. Our present data show changes in the hepatic parenchyma occurring immediately after CBDL and allow the identification of their etiopathogenesis. Our data furthermore suggest an emerging switch to more severe stages of obstructive cholestasis already 30 h after CBDL and provide an imaging method that supports and complements previous biochemical and molecular studies [13, 19, 20].

Acknowledgments

The authors kindly thank Berit Blendow, Doris Butzlaff, Dorothea Frenz, and Maren Nerowski (Institute for Experimental Surgery, University of Rostock) for excellent technical assistance. This work was supported in part by a grant from the Deutsche Forschungsgemeinschaft, Bonn, Germany (Ei 768/1–2). This funding had no impact on study design; collection, analysis and interpretation of data, or the decision to submit the paper for publication.

Disclosure Statement

All authors declare that they have no conflicts of interest.

References

1 Dooley JS: Extrahepatic biliary obstruction: systemic effects, diagnosis, management; in Bircher J, Benharnou JP, Mc Intyre N, et al (eds): Oxford Textbook of Clinical Hepatology. New York, Oxford University Press, 1999, vol 2.

2 Kinugasa T, Uchida K, Kadowaki M, Takase H, Nomura Y, Saito Y: Effect of bile duct ligation on bile acid metabolism in rats. J Lipid Res 1981;22:201–207.

3 Maillette de Buy Wenniger L, Beuers U: Bile salts and cholestasis. Dig Liver Dis 2010;42: 409–418.

4 Gressner AM: Hepatic fibrogenesis: the puzzle of interacting cells, fibrogenic cytokines, regulatory loops, and extracellular matrix molecules. Z Gastroenterol 1992;30(suppl 1):5–16.

5 Gressner AM, Bachem MG: Molecular mechanisms of liver fibrogenesis – a homage to the role of activated fat-storing cells. Digestion 1995;56:335–346.

6 Eipel C, Eisold M, Schuett H, Vollmar B: Inhibition of heme oxygenase-1 protects against tissue injury in carbon tetrachloride exposed livers. J Surg Res 2007;139:113–120.

7 Suematsu M, Oda M, Suzuki H, Kaneko H, Watanabe N, Furusho T, Masushige S, Tsuchiya M: Intravital and electron microscopic observation of Ito cells in rat hepatic microcirculation. Microvasc Res 1993;46: 28–42.

8 Haber B, Ferreira CT, Aw M, Bezerra J, Sturm E, Thompson R, D'Agostino D, McKiernan P: Cholestasis: current issues and plan for the future. J Pediatr Gastroenterol Nutr 2008;47:220–224.

9 Hirschfield GM, Heathcote EJ: Cholestasis and cholestatic syndromes. Curr Opin Gastroenterol 2009;25:175–179.

10 Popper H: Cholestasis: the future of a past and present riddle. Hepatology 1981;1:187–191.

11 Kosters A, Karpen SJ: The role of inflammation in cholestasis: clinical and basic aspects. Semin Liver Dis 2010;30:186–194.

12 Haga Y, Kay HD, Tempero MA, Zetterman RK: Flow cytometric measurement of intracellular bilirubin in human peripheral blood mononuclear cells exposed to unconjugated bilirubin. Clin Biochem 1992;25:277–283.

13 Li FC, Liu Y, Huang GT, Chiou LL, Liang JH, Sun TL, Dong CY, Lee HS: In vivo dynamic metabolic imaging of obstructive cholestasis in mice. Am J Physiol Gastrointest Liver Physiol 2009;296:G1091–G1097.

14 Lalisang TJ, Sjamsuhidajat R, Siregar NC, Taher A: Profile of hepatocyte apoptosis and bile lakes before and after bile duct decompression in severe obstructive jaundice patients. Hepatobiliary Pancreat Dis Int 2010; 9:520–523.

15 Shibayama Y: Factors producing bile infarction and bile duct proliferation in biliary obstruction. J Pathol 1990;160:57–62.

16 Friedman SL: Seminars in medicine of the Beth Israel Hospital, Boston. The cellular basis of hepatic fibrosis. Mechanisms and treatment strategies. N Engl J Med 1993;328: 1828–1835.

17 Jiao J, Friedman SL, Aloman C: Hepatic fibrosis. Curr Opin Gastroenterol 2009;25: 223–229.

18 Mathew J, Geerts A, Burt AD: Pathobiology of hepatic stellate cells. Hepatogastroenterology 1996;43:72–91.

19 Denk GU, Soroka CJ, Takeyama Y, Chen WS, Schuetz JD, Boyer JL: Multidrug resistance-associated protein 4 is up-regulated in liver but down-regulated in kidney in obstructive cholestasis in the rat. J Hepatol 2004;40:585–591.

20 Mennone A, Soroka CJ, Cai SY, Harry K, Adachi M, Hagey L, Schuetz JD, Boyer JL: Mrp4–/– mice have an impaired cytoprotective response in obstructive cholestasis. Hepatology 2006;43:1013–1021.